Physics in Medicine & Biology

IPEM Institute of Physics and Engineering in Medicine

Refractive indices of human skin tissues at eight wavelengths and estimated dispersion relations between 300 and 1600 nm

To cite this article: Huafeng Ding *et al* 2006 *Phys. Med. Biol.* **51** 1479

View the article online for updates and enhancements.

Related content

- Optical properties of porcine skin dermis between 900 nm and 1500 nm
Y Du, X H Hu, M Cariveau et al.
- Optical properties of human skin, subcutaneous and mucous tissues in the wavelength range from 400 to 2000 nm
A N Bashkatov, E A Genina, V I Kochubey et al.
- Determination of complex refractive index of polystyrene microspheres from 370 to 1610 nm
Xiaoyan Ma, Jun Q Lu, R Scott Brock et al.

Recent citations

- Extended derivative method of critical-angle refractometry for attenuating media: error analysis
Spyridon Koutsoumpos *et al*
- A Weighted Average Phase Velocity Inversion Model for Depth-Resolved Elasticity Evaluation in Human Skin In-Vivo
Kanheng Zhou *et al*
- Parametric handheld optical probe (HOPE) for biological tissue characterization in the near-infrared spectral range
Daniel Davidov *et al*

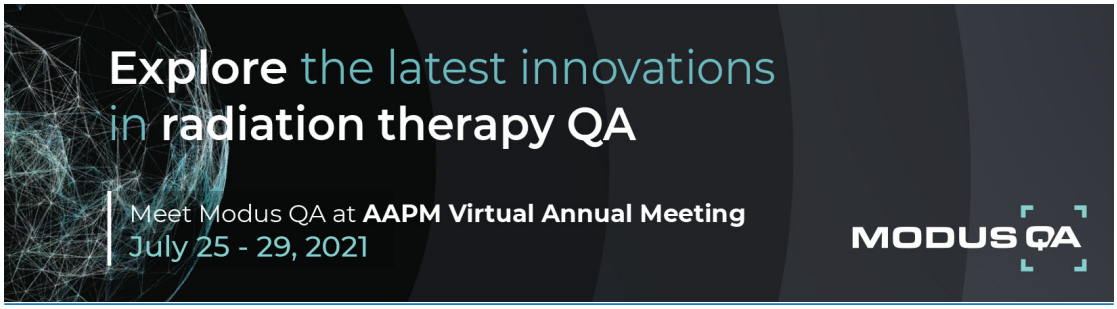

This content was downloaded from IP address 132.174.251.2 on 24/07/2021 at 18:47

DOCKET ALARM

Find authenticated court documents without watermarks at docketalarm.com.

INSTITUTE OF PHYSICS PUBLISHING PHYSICS IN MEDICINE AND BIOLOGY

Phys. Med. Biol. **51** (2006) 1479–1489 doi:10.1088/0031-9155/51/6/008

Refractive indices of human skin tissues at eight wavelengths and estimated dispersion relations between 300 and 1600 nm

Huafeng Ding[1], Jun Q Lu[1], William A Wooden[2], Peter J Kragel[3] and Xin-Hua Hu[1]

[1] Department of Physics, East Carolina University, Greenville, NC 27858, USA
[2] Department of Surgery, Brody School of Medicine, East Carolina University, Greenville, NC 27858, USA
[3] Department of Pathology, Brody School of Medicine, East Carolina University, Greenville, NC 27858, USA

E-mail: hux@ecu.edu

Received 7 September 2005, in final form 3 January 2006
Published 1 March 2006
Online at stacks.iop.org/PMB/51/1479

Abstract

The refractive index of human skin tissues is an important parameter in characterizing the optical response of the skin. We extended a previously developed method of coherent reflectance curve measurement to determine the *in vitro* values of the complex refractive indices of epidermal and dermal tissues from fresh human skin samples at eight wavelengths between 325 and 1557 nm. Based on these results, dispersion relations of the real refractive index have been obtained and compared in the same spectral region.

(Some figures in this article are in colour only in the electronic version)

1. Introduction

Understanding the response of the skin to optical radiation is essential to the dermatological applications of photomedicine. Among various skin optical parameters, refractive index is an important one. At the microscopic scales ranging from 1 to 10 μm, refractive index variation causes light scattering which can be understood by direct solution of the Maxwell equations within the framework of classical electrodynamics for simple shaped particles (Bohren and Huffman 1983, Ma *et al* 2003a) and for biological cells (Lu *et al* 2005). For highly turbid tissues of human skin with sizes of 1 mm or larger, modelling of tissue optics based on the electrodynamic theory is very difficult, and the real refractive index and scattering parameters are often treated as independent parameters within the frameworks of effective medium theory and radiative transfer theory, respectively. For example, in the widely used method of Monte Carlo simulation of light distribution in biological tissues, photon interaction with an interface

DOCKET ALARM Find authenticated court documents without watermarks at docketalarm.com.

between tissue regions of different refractive indices is described according to the Fresnel equations which require the index as the key parameter (van Gemert *et al* 1989, Wang *et al* 1995, Lu *et al* 2000). Furthermore, accurate modelling of measured light signals near a skin surface requires the refractive indices of skin tissues to account for the redistribution of light due to the index mismatch at the surface (Lu *et al* 2000, Meglinsky and Matcher 2001, Bartlett and Jiang 2001, Ma *et al* 2003b, 2005).

Determination of the refractive indices of the human skin tissues, however, presents challenges because of their highly turbid natures. In transparent or absorbing media such as the aqueous solutions with molecular solutes, propagation of light is dominated by its coherent component. The reflection and refraction of a light beam, as it passes through an interface between two media of different refractive indices, are described with the Fresnel equations on the basis of an effective medium theory. In contrast, light propagation in a turbid medium produces a scattering component that becomes increasingly dominant as the light penetrates into the medium. This feature of interaction often precludes the use of refraction method to determine the refractive index of biological tissue samples where uniform and thin samples are very difficult to obtain. Recently, we developed an automated reflectometer system for determining the refractive index of a turbid sample by measurement of its coherent reflectance R versus the incident angle θ without the need to section skin tissues (Ding *et al* 2005). Here we report complex refractive indices of fresh human skin tissues determined by nonlinear regression of $R(\theta)$ with the Fresnel equations. The complex refractive index has been obtained at eight wavelengths between 325 and 1557 nm for both the epidermis and dermis tissues. With these data we investigated various dispersion schemes for interpolation of the index data at other wavelengths in this spectral region.

2. Methods

Fresh skin tissue patches were obtained from the patients undergoing abdominoplasty procedures at the plastic surgery clinic of the Brody School of Medicine, East Carolina University (ECU). A study protocol approved by the Institutional Review Board of ECU was strictly followed and a consent form was signed by each participating patient before the surgery. We obtained one skin tissue patch from each of the 12 female patients with ages between 27 and 63 years old; 10 are Caucasian and 2 are African Americans, with the skin data compiled in table 1. Each skin patch was stored in a bucket on crushed ice (~2 °C) inside a refrigerator immediately after surgery. Samples with sizes of about 1 cm × 1 cm were prepared by removing the hair on the skin surface with scissors and subcutaneous fat tissue with a razor blade and warming the skin to a room temperature of about 22 °C with 0.9% saline drops. Care was taken to preserve the stratum corneum layer of the skin epidermis. The skin sample was pressed against the base of the prism with a pistol pressurized by a nitrogen gas cylinder to maintain good contact between the sample and the prism. The periphery of the tissue sample between the pistol and prism base was sealed with plastic tape to prevent sample dehydration during the measurement. By pressing either the epidermis or dermis side of the skin sample against the prism base, the coherent reflectance curves of skin epidermis or dermis were measured, respectively. All reflectance curve measurements were performed at the room temperature within 30 h after the abdominoplasty procedure.

An automated reflectometer system has been designed and constructed to measure the coherent reflectance as a function of incident angle. Compared to other approaches of index determination based on fibre insertion and OCT (Bolin *et al* 1989, Tearney *et al* 1995, Knuttel and Boehlau-Godau 2000), this method has the combined benefits of high accuracy, wide spectral capability and instrumentation simplicity. The system has been described in detail

DOCKET ALARM Find authenticated court documents without watermarks at docketalarm.com.

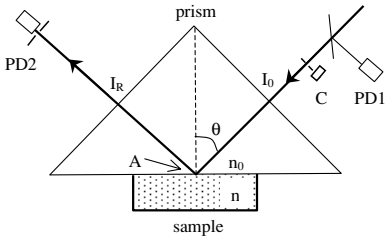

Figure 1. The schematic of the reflectomer system.

Table 1. The human skin sample data.

ID no.	Age	Race	Tissue location	Skin type	Measurement
1	42	Caucasian	Abdomen	III	Pressure dependence
2	40	Caucasian	Abdomen	I	633 nm, 532 nm
3	27	African American	Abdomen	V	442 nm
4	63	Caucasian	Abdomen	II	1064, 850 nm
5	56	Caucasian	Abdomen	II	325,1550 nm
6	54	Caucasian	Arm	II	1310, 633 nm
7	34	Caucasian	Abdomen	II	1064, 325 nm
8[a]	55	Caucasian	Abdomen	I	532,633 nm
9[a]	49	Caucasian	Abdomen	III	442,1310 nm
10[a]	41	Caucasian	Abdomen	II	850,1550 nm
11[a]	39	African American	Abdomen	V	532, diffuse reflection
12	44	Caucasian	Abdomen	III	Pressure dependence

[a] The skin structures of the samples from these patients have been examined through histology.

elsewhere (Ding *et al* 2005). Briefly, a right-angle glass prism was used to interface with a skin sample on the prism base and a linear polarized laser beam was propagated through one side surface as the incident beam on the prism–sample interface at an incident angle of θ. The coherent reflectance R of the laser beam was measured at the angle of specular reflection by a photodiode of either Si or GaAs, depending on the light wavelength. Two coherent reflectance curves, $R_s(\theta)$ or $R_p(\theta)$, have actually been measured for each sample with either s- or p-polarized incident beam, respectively. The incident angle θ can be varied between 48° and 80° with a stepsize of 0.125° and resolution of 0.006°. A schematic diagram of the optical setup is presented in figure 1. The powers of the incident and reflected beams were measured by two identical photodiodes and the effect of the reflection loss at the side surfaces of the prism was removed to determine the coherent reflectance (R_s or R_p). To reduce the contribution of diffuse reflection to reflection signal, a pinhole of 2 mm diameter was used in front of the photodiode, resulting in an angular range of 1.74×10^{-2} rad or about 1.00° in the measurement. The incident laser beam, modulated at 370 Hz for lock-in detection, was produced by one of seven continuous-wave (cw) lasers at one of eight wavelengths: $\lambda = 325$, 442, 532, 633, 850, 1064, 1310 and 1557 nm. The diameter of the beam was set to between 1 and 2 mm with the incident beam power adjusted to be about 1 μW.

The measured coherent reflectance curves have been fitted by the calculated values, $\tilde{R}_s(\theta)$ and $\tilde{R}_p(\theta)$, according to the Fresnel equations. The fitting requires the assumed value of the

DOCKET ALARM
Find authenticated court documents without watermarks at docketalarm.com.

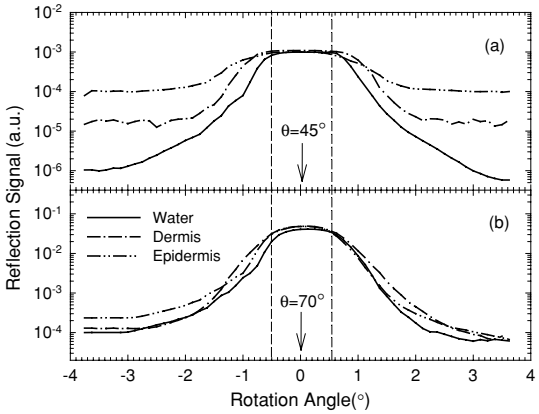

Figure 2. The reflection signal versus rotation angle of the detector at the incident angle of (a) $\theta = 45^\circ$; (b) $\theta = 70^\circ$ with a s-polarized beam at $\lambda = 633$ nm for deionized water, the epidermis and dermis of one skin sample. The error bars of about $\pm 5\%$ were removed for clear view and the two dashed lines indicate the angular acceptance range of the aperture in front of the photodiode.

complex refractive index of the turbid sample, $n = n_r + in_i$, and the known refractive index, n_0, of the prism. Therefore, the index n was inversely determined using an iteration process to achieve least-squared difference between the calculated and measured curves (Ding *et al* 2005). The consistency between the measured and calculated coherent reflectance curves is described by a coefficient of determination, R^2, defined as

$$R^2 = 1 - \frac{\sum_{i=1}^{N} (R_i - \tilde{R}_i)^2}{\sum_{i=1}^{N} (R_i - \bar{R})^2}, \tag{1}$$

where R_i and $\tilde{R}_i$ denote the measured and calculated reflectances at the ith angle of incidence θ_i, respectively, and $\bar{R}$ is the mean value of measured reflectance over N values of θ. The R^2 value ranges between 0 and 1 with $R^2 = 1$ for a perfect fit. The system was calibrated before measurements of each sample by comparing the measured real refractive index of deionized water with the published value at the wavelength of measurements (Hale and Querry 1973). From the water data, the experimental error in determination of the real refractive index n_r of transparent samples by the reflectometer system was found to be about $\delta n_r = \pm 0.002$.

3. Results

To ensure that the reflection signal is dominated by its coherent component, we measured the angular distribution of the reflected beam around a specular reflection angle at two positions ($\theta = 45^\circ$ or 75°) with $\lambda = 633$ nm. Similar data with deionized water were used as the baseline and all are plotted in figure 2. These results demonstrate that the contribution of the diffusely reflected light to the coherent reflectance signal is negligible within the 1° angular range defined by the photodiode aperture (indicated by the dashed lines in figure 2). Two typical sets of coherent reflectance curves from the epidermis and dermis sides of the skin

DOCKET ALARM
Find authenticated court documents without watermarks at docketalarm.com.

DOCKET ALARM

Explore Litigation Insights

Docket Alarm provides insights to develop a more informed litigation strategy and the peace of mind of knowing you're on top of things.

Real-Time Litigation Alerts

Keep your litigation team up-to-date with **real-time alerts** and advanced team management tools built for the enterprise, all while greatly reducing PACER spend.

Our comprehensive service means we can handle Federal, State, and Administrative courts across the country.

Advanced Docket Research

With over 230 million records, Docket Alarm's cloud-native docket research platform finds what other services can't. Coverage includes Federal, State, plus PTAB, TTAB, ITC and NLRB decisions, all in one place.

Identify arguments that have been successful in the past with full text, pinpoint searching. Link to case law cited within any court document via Fastcase.

Analytics At Your Fingertips

Learn what happened the last time a particular judge, opposing counsel or company faced cases similar to yours.

Advanced out-of-the-box PTAB and TTAB analytics are always at your fingertips.

API

Docket Alarm offers a powerful API (application programming interface) to developers that want to integrate case filings into their apps.

LAW FIRMS
Build custom dashboards for your attorneys and clients with live data direct from the court.

Automate many repetitive legal tasks like conflict checks, document management, and marketing.

FINANCIAL INSTITUTIONS
Litigation and bankruptcy checks for companies and debtors.

E-DISCOVERY AND LEGAL VENDORS
Sync your system to PACER to automate legal marketing.